Contribution from the Division of Biological Sciences, National Research Council of Canada,
Ottawa, Canada K1A 0R6, and Department of Chemistry, University of Ottawa, Ottawa, Canada K1N 9B4

Structure of Bis(triphenylphosphine)dicarbonylnitrosyliron Tetrafluoroborate–Dichloromethane and Correlation of the Fe–P Bond Length with the Degeneracy-Weighted Stretching Frequency of CO[1]

F. R. AHMED,*[2a] J. L. A. ROUSTAN,*[2b] and M. Y. AL-JANABI[2b,c]

Received August 10, 1984

The complex $[Fe(P(C_6H_5)_3)_2(CO)_2(NO)]^+[BF_4]^-\cdot CH_2Cl_2$ crystallizes in the monoclinic system, space group $P2_1/n$ with $a = 17.247$ (3) Å, $b = 13.754$ (2) Å, $c = 16.914$ (2) Å, $\beta = 104.26$ (1)°, $V = 3888.6$ Å^3, and $Z = 4$. The structure has been refined to $R = 0.045$, $R_w = 0.052$ for 4195 reflections with $I \geq 2.0\sigma(I)$. The coordination around the Fe atom is trigonal bipyramidal with the dicarbonyl and nitrosyl in the basal plane and the two P atoms in apical positions. The $(CO)_2$ and NO positions appear to be interchanged in the different molecules. The tetrafluoroborate and dichloromethane are situated in channels with disordered orientations. The mean Fe–P bond length and P–Fe–P angle are 2.280 (3) Å and 177.45 (5)° in the title compound, compared to 2.182 (7) Å and 140.9 (1)° in $FeH(P(C_6H_5)_3)_2(CO)(NO)$, respectively. In these two complexes and in $Fe(CO)_4(P(C_6H_5)_3)$ and $[Fe(CO)_2(N_2C_6H_5)(P(C_6H_5)_3)_2]^+$, which are trigonal-bipyramidal d^8 complexes, the mean Fe–P bond length is shown to increase linearly with the degeneracy-weighted stretching frequency of the carbonyl group, $\langle\nu(CO)\rangle$. The same correlation persists, but with a wider spread of ±0.02 Å, when a selection of 22 iron carbonyl triphenylphosphine complexes are examined. A similar pattern also is observed for a limited series of trigonal-bipyramidal d^8 Mn complexes.

Introduction

Protonation of the anion in $Fe(CO)_3(NO)^-Na^+$ in the presence of triphenylphosphine was found to yield the iron nitrosyl hydride $FeH(CO)(NO)(PPh_3)_2$ (**1**), whose structure has been determined recently.[3] Upon suitable modification of the experimental conditions, the protonation reaction can be diverted to produce the iron nitrosyl cation $[Fe(CO)_2(NO)(PPh_3)_2]^+$ (**2**).[4] It was anticipated that comparison of the structures of **1** and **2** would provide valuable information on the relative influences of basal H$^-$ and CO ligands on the axial phosphine bond lengths in pentacoordinated complexes of a first-row element. In this paper, we report the crystal structure of the tetrafluoroborate–dichloromethane complex of **2**. For analysis of the factors that may control the Fe–P bond lengths in **1** and **2**, it was necessary to consider a wide selection of iron carbonyl triphenylphosphine complexes, as well as a few manganese complexes. The results of these investigations are presented and discussed.

Experimental Section

Preparation of the Complex. The cation $[Fe(CO)_2(NO)(PPh_3)_2]^+$ (**2**) was isolated as the tetrafluoroborate salt by protonation of a mixture of $Fe(CO)_3(NO)^-Na^+$ and PPh_3 in THF with HBF_4, as described previously.[4]

Single crystals of the complex were grown under argon at room temperature by slow diffusion of an upper layer of hexane into a concentrated solution of the BF_4^- salt of **2** in CH_2Cl_2.

Crystallographic Data. The X-ray data were measured from a light brown crystal in the shape of an approximate cube, 0.37 × 0.37 × 0.40 mm, on an Enraf-Nonius CAD-4 diffractometer using Zr-filtered Mo Kα radiation at 296 K. The cell parameters were derived by least squares from the angular settings of 22 reflections in the range $15 < \theta \leq 18°$, and the crystal density was measured by flotation in aqueous KI solution. Intensities for hkl and $\bar{h}kl$ to $2\theta = 50°$ were obtained by ω–2θ scans with $\Delta\omega = 1.5(0.9 + 0.35 \tan\theta)°$ and a horizontal aperture equal to $(4 + 0.4 \tan\theta)$ mm. Three standard reflections, which were monitored every hour, varied by only ±1.2% from the mean. Of 6820 unique reflections measured, 4195 with $I \geq 2.0\sigma(I)$ were considered observed. The intensities were corrected for background, the small scale variations, and Lorentz and polarization effects but not for extinction or absorption (transmission factors 0.65–0.78). The crystal data are summarized in Table I.

Table I. Crystal Data and Refinement Indicators for $[C_{38}H_{30}FeNO_3P_2]BF_4\cdot CH_2Cl_2$

fw	838.19	radiation	Mo Kα
cryst syst	monoclinic	λ, Å	0.71069
space group	$P2_1/n$	μ, cm^{-1}	6.61
a, Å	17.247 (3)	$2\theta_{max}$, deg	50
b, Å	13.754 (2)	measd reflecns	6820
c, Å	16.914 (2)	obsd reflecns (m)^a	4195
β, deg	104.26 (1)	parameters varied (n)	522
V, Å^3	3888.6	R^b	0.045
Z	4	$R_w{}^c$	0.052
D_{calcd}, g cm^{-3}	1.431	GOF^d	1.46
D_{obsd}, g cm^{-3}	1.430	max (Δ/σ) ordered atoms	0.18
$F(000)$	1712	max (Δ/σ) disordered atoms	1.61

$^a I \geq 2.0\sigma(I)$. $^b R = \sum[|F_o| - |F_c|]/\sum|F_o|$. $^c R_w = [\sum w(|F_o| - |F_c|)^2/\sum w|F_o|^2]^{1/2}$. $^d \mathrm{GOF} = [\sum w(|F_o| - |F_c|)^2/(m - n)]^{1/2}$.

Structure Determination and Refinement. The Fe and P positions were derived from a sharpened Patterson map, and the other atoms were located from Fourier and difference maps. Disorder was indicated for the two Cl and three of the F atoms, with approximate occupancies of 0.5 each. Also, the $(CO)_2$ and NO appeared to be interchanged in the different molecules, necessitating the use of a composite CN scattering factor curve calculated as $f_{CN} = (2f_C + f_N)/3$ for the three C/N positions. Attempts at refining the occupancies of the CN positions produced insignificant shifts, $< \pm 1.5\sigma$, which could not be accepted for clear identification of the NO group. These occupancy parameters then were fixed at 1.0 in the last two cycles, since the corresponding bond lengths also lent support to the assumption of C/N interchange. Positional and anisotropic thermal parameters for the non-hydrogen atoms, including the disordered F and Cl, were refined by block-diagonal least squares minimizing $\sum w(|F_o| - |F_c|)^2$ with $w = [1 + ((|F_o| - 35)/30^2)]^{-1}$ in the final cycles. The H atoms, except those of CH_2Cl_2, were identified from difference maps but their parameters were not refined, and their temperature factors were fixed at 4.0 Å^2. The three reflections 011, $\bar{1}01$, and $\bar{2}04$ showing high discrepancies were assigned zero weights. The first two are close to the direct beam, $2\theta < 4°$, while the third is the strongest in the dataset and shows extinction effect. Convergence was reached at $R = 0.045$ and $R_w = 0.052$ for the 4195 observed reflections, where the residual electron density was within −0.36 and 0.30 e Å^{-3} in the final difference map. Other refinement indicators are included in Table I. Scattering factors for the neutral atoms, ignoring the anomalous dispersion contribution, were from ref 5 and 6 and the computations were done by using the NRC program system[7] and ORTEP.[8] The refined atomic parameters are listed in Table II. Observed and calculated

---

[1] Issued as NRCC Publication No. 24617.

[2] (a) National Research Council of Canada. (b) University of Ottawa. (c) On sabbatical leave from the College of Education, University of Baghdad, Iraq, during the year 1979–1980.

[3] Cygler, M.; Ahmed, F. R.; Forgues, A.; Roustan, J. L. A. *Inorg. Chem.* **1983**, *22*, 1025.

[4] Roustan, J. L. A.; Forgues, A.; Venayak, D.; Merour, J. Y.; Morrow, B. *Can. J. Chem.* **1983**, *61*, 1339.

[5] "International Tables for X-ray Crystallography"; Kynoch Press: Birmingham, England, 1974; Vol. IV, p 73.

[6] Stewart, R. F.; Davidson, E. R.; Simpson, W. T. *J. Chem. Phys.* **1965**, *42*, 3175.

[7] Ahmed, F. R.; Hall, S. R.; Pippy, M. E.; Huber, C. P. NRC Crystallographic Programs for the IBM/360 System Accession Nos. 133–147 in: *J. Appl. Crystallogr.* **1973**, *6*, 309.

[8] Johnson, C. K. "ORTEP", Report ORNL-3794; Oak Ridge National Laboratory: Oak Ridge, TN, 1965.

0020-1669/85/1324-2526$01.50/0 Published 1985 by the American Chemical Society

Table II. Atomic Parameters (×10^5 for Fe; ×10^4 for Other Atoms) and Their Estimated Standard Deviations

	x	y	z	B_{eq}[a]
Fe	−8634 (4)	15218 (4)	15648 (4)	3.1
P(1)	−10973 (6)	1147 (7)	21821 (6)	2.7
P(2)	−5721 (6)	29234 (7)	9808 (6)	2.8
CN(1)	−1674 (2)	2087 (3)	1842 (2)	3.6
CN(2)	−1034 (2)	925 (3)	620 (2)	3.5
CN(3)	116 (2)	1547 (3)	2206 (2)	4.0
O(1)	−2202 (2)	2453 (3)	2007 (2)	6.5
O(2)	−1152 (2)	539 (3)	7 (2)	6.0
O(3)	751 (2)	1550 (3)	2593 (2)	6.5
C(11)	−1291 (2)	297 (3)	3180 (2)	3.0
C(12)	−739 (3)	786 (3)	3776 (3)	4.0
C(13)	−832 (3)	855 (3)	4560 (3)	4.2
C(14)	−1489 (3)	451 (4)	4754 (3)	4.7
C(15)	−2054 (3)	−1 (4)	4161 (3)	5.4
C(16)	−1964 (3)	−89 (3)	3374 (3)	4.1
C(21)	−1936 (2)	−591 (3)	1603 (2)	3.1
C(22)	−2612 (3)	−126 (3)	1154 (3)	4.1
C(23)	−3274 (3)	−659 (4)	765 (3)	4.7
C(24)	−3267 (3)	−1657 (4)	826 (3)	5.0
C(25)	−2606 (3)	−2128 (3)	1254 (3)	4.9
C(26)	−1931 (3)	−1601 (3)	1653 (3)	4.1
C(31)	−244 (2)	−699 (3)	2376 (2)	3.2
C(32)	228 (3)	−770 (4)	1821 (3)	5.0
C(33)	889 (4)	−1390 (5)	1967 (3)	6.6
C(34)	1064 (3)	−1936 (4)	2667 (3)	6.1
C(35)	600 (3)	−1900 (4)	3207 (3)	5.2
C(36)	−60 (3)	−1278 (3)	3077 (3)	4.2
C(41)	−1231 (2)	3180 (3)	−14 (2)	3.2
C(42)	−2051 (3)	3040 (4)	−138 (3)	4.4
C(43)	−2565 (3)	3286 (4)	−877 (3)	5.3
C(44)	−2262 (3)	3667 (4)	−1493 (3)	5.2
C(45)	−1457 (3)	3801 (3)	−1380 (3)	4.9
C(46)	−935 (3)	3559 (3)	−641 (3)	4.1
C(51)	423 (2)	2900 (3)	800 (2)	3.1
C(52)	671 (3)	2109 (4)	426 (3)	5.6
C(53)	1410 (3)	2079 (4)	261 (4)	6.4
C(54)	1933 (3)	2843 (4)	489 (3)	5.5
C(55)	1694 (3)	3642 (4)	843 (4)	6.0
C(56)	939 (3)	3662 (3)	1005 (3)	4.9
C(61)	−609 (2)	4012 (3)	1586 (2)	3.1
C(62)	−448 (3)	3960 (3)	2428 (3)	4.3
C(63)	−460 (3)	4803 (4)	2885 (3)	5.6
C(64)	−635 (3)	5690 (4)	2496 (3)	5.8
C(65)	−784 (3)	5742 (3)	1665 (3)	5.4
C(66)	−774 (3)	4911 (3)	1200 (3)	4.3
B	5745 (4)	2027 (6)	59 (4)	6.3
F(1)	6513 (2)	1738 (3)	248 (3)	9.1
C(1)	1758 (5)	4542 (6)	3781 (4)	8.6
F(12)[b]	5401 (5)	2011 (8)	−708 (5)	11.5
F(13)[b]	5252 (5)	1792 (9)	466 (5)	12.4
F(14)[b]	5901 (6)	3053 (6)	231 (8)	12.9
F(22)[b]	5462 (6)	2445 (8)	580 (6)	12.6
F(23)[b]	5593 (5)	2501 (8)	−661 (6)	11.5
F(24)[b]	5368 (5)	1080 (6)	−90 (7)	11.9
Cl(11)[b]	1795 (2)	3844 (3)	2939 (3)	9.4
Cl(12)[b]	2160 (4)	4112 (4)	3031 (3)	15.5
Cl(21)[b]	2157 (3)	5673 (3)	3702 (3)	11.1
Cl(22)[b]	1541 (3)	5778 (3)	3638 (2)	9.1

[a] $B_{eq} = (8/3)\pi^2\sum_i\sum_j U_{ij}a_i{}^*a_j{}^*\mathbf{a}_i\cdot\mathbf{a}_j$ Å^2. [b] Occupancy 0.5.

structure amplitudes, parameters for the H atoms, U_{ij}'s for the non-hydrogen atoms, and the geometries of the phenyl rings, disordered BF_4, and CH_2Cl_2 have been deposited as supplementary material.

Infrared Data. The degeneracy weighted stretching frequencies $\langle\nu(CO)\rangle$'s for the compounds listed in Tables V and VI were calculated as in ref 9. As an example, the IR data for $Fe(CO)_4(PPh_3)$ (**6**)[10] yield $\langle\nu(CO)\rangle = {}^1/_4[2050.5(A_1{}^{(2)}) + 1977.3(A_1{}^{(1)}) + 2 \times 1945.2(E)] \simeq 1980$ cm^{-1}. For $Fe(CO)_3(\eta^2$-diethyl fumarate$)(PPh_3)$ (**8**) and $Fe(CO)_3(\eta^2$-diethyl maleate$)(PPh_3)$ (**9**), the $\langle\nu(CO)\rangle$'s of 2009 and 1995 cm^{-1}, respectively, were calculated from the IR spectra (CH_2Cl_2) kindly provided by Professor J. Takats. In each case, three infrared-active $\nu(CO)$'s were present, as expected for a local symmetry of C_{2v} and **8** and C_s for **9** suggested by the solid-state structures.[11] The relative intensities also were in the appropriate order as found by comparing the spectra with those of other $M(CO)_3$ complexes having the same local symmetries.[12] $Fe(CO)_3(\eta^2$-methyl acrylate$)(PPh_3)$ (**10**) has a single-crystal X-ray structure similar to that of **9** with an apical phosphine.[13] However, the reported $\nu(CO)$'s[14] exceed the number of vibrations expected, indicating the possible existence in solution of more than one isomer. By comparison with the spectrum of **9**, the tentative assignments considered for the nondegenerated $\nu(CO)$'s of **10** were 2042.5 or 2035 cm^{-1}, 1981 or 1975 cm^{-1}, and 1945 cm^{-1}. That led to $\langle\nu(CO)\rangle$ values in the range 1985–1989.5 cm^{-1}. An intermediate value of 1987 cm^{-1} was used to locate **10** in the plot of Figure 4. However, inclusion or omission of this point has no significant effect on the results of the correlations between

Table III. Selected Bond Lengths (Å) and Valence Angles (deg)

Fe–P(1)	2.282 (1)	P(1)–Fe–P(2)	177.45 (5)
Fe–P(2)	2.278 (1)	P(1)–Fe–CN(1)	90.6 (1)
Fe–CN(1)	1.761 (4)	P(1)–Fe–CN(2)	90.6 (1)
Fe–CN(2)	1.756 (4)	P(1)–Fe–CN(3)	89.2 (1)
Fe–CN(3)	1.769 (4)	P(2)–Fe–CN(1)	90.9 (1)
CN(1)–O(1)	1.134 (5)	P(2)–Fe–CN(2)	90.4 (1)
CN(2)–O(2)	1.138 (5)	P(2)–Fe–CN(3)	88.3 (1)
CN(3)–O(3)	1.129 (5)	CN(1)–Fe–CN(2)	118.9 (2)
P(1)–C(11)	1.817 (4)	CN(1)–Fe–CN(3)	121.9 (2)
P(1)–C(21)	1.815 (4)	CN(2)–Fe–CN(3)	119.2 (2)
P(1)–C(31)	1.813 (4)	Fe–CN(1)–O(1)	178.8 (4)
P(2)–C(41)	1.818 (4)	Fe–CN(2)–O(2)	179.4 (4)
P(2)–C(51)	1.816 (4)	Fe–CN(3)–O(3)	177.5 (4)
P(2)–C(61)	1.824 (4)		

	range	mean[a]
C–C	1.355 (7)–1.398 (6)	1.381 [12]
B–F	1.25 (1)–1.45 (1)	1.34 [8]
C–Cl	1.695 (10)–1.745 (9)	1.723 [21]
C–H	0.86–1.13	0.99 [8]
Fe–P–C	112.1 (1)–114.4 (1)	113.5 [10]
C–P–C	104.1 (2)–105.9 (2)	105.2 [8]
P–C–C	119.6 (3)–121.9 (3)	120.5 [7]
C–C–C	117.8 (4)–121.8 (5)	120.0 [8]
F–B–F[b]	96.7 (6)–123.5 (8)	109.1 [80]
Cl–C–Cl	109.9 (5)–110.5 (5)	110.2 [4]

[a] See ref 18. [b] For terminal atoms of the same (disordered) unit.

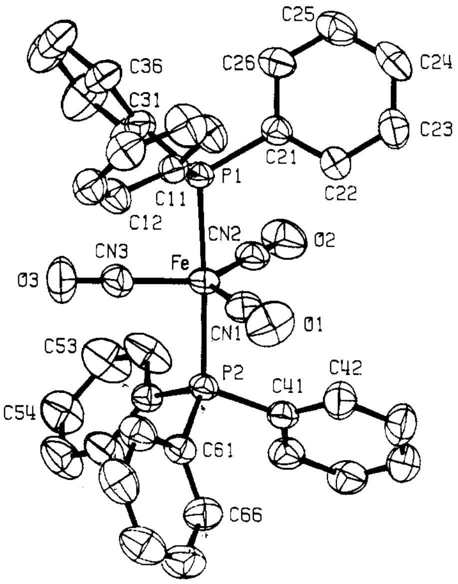

Figure 1. An ORTEP orthogonal projection of the molecular structure of the cation showing the ellipsoids of thermal vibration drawn at 50% probability.

---

(9) Avanzino, S. C.; Bakke, A. A.; Chen, H. W.;Donahue, C. J.; Jolly, W. L.; Lee, J. H.; Ricco, A. J. *Inorg. Chem.* **1980**, *19*, 1931.

(10) Darenbourg, D. J.; Nelson, H. H.; Hyde, C. L. *Inorg. Chem.* **1974**, *13*, 2135.

(11) Stainer, M. V. R.; Takats, T. J. *Inorg. Chem.* **1982**, *21*, 4044.

(12) Angelici, R. J.; Basolo, F.; Poë, A. J. *J. Am. Chem. Soc.* **1963**, *85*, 2215.

(13) Krüger, C.; Tsay, Y. H. *Cryst. Struct. Commun.* **1976**, *5*, 219.

(14) Grevels, F. W.; Schulz, D.; Koerner Von Gustorf, E. *Angew. Chem., Int. Ed. Engl.* **1974**, *13*, 534.

Table IV. Comparison of Valence Angles (deg) in the Iron Cation with Those of Closely Related Os and Mn Complexes

	$[Fe(CO)_2(NO)(P(C_6H_5)_3)_2]^+$ (**2**)[a]	$[Os(CO)_2(NO)(P(C_6H_5)_3)_2]^+$ (**3**)[b]	$Mn(CO)_2(NO)(P(C_6H_5)_3)_2$ (**4**)[c]
P–M–P	177.45 (5)	177.96 (8)	170.2 (2)
P–M–CN	90.6 (1), 90.6 (1), 89.2 (1) 90.9 (1), 90.4 (1), 88.3 (1)	90.1 (3), 91.1 (3), 89.3 (3) 91.0 (3), 90.0 (3), 88.6 (3)	86.2 (5), 89.4 (5), 94.5 (4) 85.5 (5), 90.1 (5), 94.1 (4)
CN–M–CN	118.9 (2), 119.2 (2), 121.9 (2)	115.2 (5), 119.5 (5), 125.3 (5)	118.7 (7), 120.0 (7), 121.3 (7)
M–CN–O	177.5 (4), 178.8 (4), 179.4 (4)	178.0 (10), 178.2 (10), 178.7 (10)	177.4 (17), 178.0 (13), 178.2 (18)
C–P–C (range)	104.1 (2)–105.9 (2)	103.9 (4)–106.3 (4)	100.8 (8)–105.0 (6)
M–P–C (range)	111.1 (1)–114.4 (1)	111.5 (3)–114.7 (3)	114.1 (5)–118.0 (4)

[a] This work. [b] Reference 15. [c] Reference 16.

Table V. Bond Lengths (l(Fe–P), Å) with Esd's in Parentheses and Degeneracy-Weighted Stretching Frequencies (⟨2(CO)⟩, cm^{-1}) of Iron Carbonyl Triphenylphosphine Complexes

no.	complex[a]	l(Fe–P)[b]	ref	⟨ν(CO)⟩	ref
1	$Fe(CO)(NO)(L)_2H$	2.188 (2); 2.188 (2) 2.179 (2); 2.174 (2) {2.182} [7]	3	1910	3
2	$[Fe(CO)_2(NO)(L)_2]^+$	2.282 (1); 2.278 (1) {2.280} [3]	this work	2022	60
5	$[Fe(CO)_2(N_2Ph)(L)_2]^+$	2.266 (2); 2.261 (2) {2.264} [4]	19	2004	61
6	$Fe(CO)_4(L)$	2.244 (1)	62	1980	10
7	$Fe(CO)_2(CS_2)(PMe_3)(L)$	2.279 (1)	63	1964	63
8	$Fe(CO)_3(\eta^2\text{-DEF})(L)$	2.274 (1)	11	2009	64
9	$Fe(CO)_3(\eta^2\text{-DEM})(L)$	2.286 (1)	11	1995	64
10	$Fe(CO)_3(\eta^2\text{-MA})(L)$	2.275 (1)	13	1987[d]	14
11	$Fe(CO)_2(\eta^4\text{-TAC})(L)$	2.238 (2)	65	1958[c]	66
12	$Fe(CO)_2(\eta^4\text{-PhCHCHCHO})(L)$	2.257 (1)	67	1968	68
13	$Fe(CO)_2(\eta^4\text{-1,2-cyclohex})(L)$	2.232 (1)	69	1940	69
14	$Fe(CO)_2(\eta^4\text{-1-MeO-1,2-cyclohex})(L)$	2.225 (1)	69	1939	69
15	$Fe(CO)(NO)_2(L)$	2.260 (3)	20	2010	70
16	$Fe(CO)_2(\eta^3\text{-C(O)C(OMe)C(CO}_2\text{Me)CH}_2)(L)$	2.247 (2)	71	1994	71
17	$Fp'(CH_2CO_2ment)(L)$	2.198 (3); 2.193 (4) {2.196} [4]	72	1930	73
18	$Fp'(C(CO_2Et)CMe_2)(L)$	2.2236 (6)	53	1925	53
19	$Fp'(SO_2CH_2CHMe)_2(L)$	2.237 (2)	74	1950	73
20	$Fp'(CH_2Oment)(L)$	2.181 (2)	72	1900	73
21	$Fp'(CO_2ment)(L)$	2.214 (2)	48	1938	75
22	$[Fp'(C(PPh_3)CH_2)(L)]^+[BF_4]^-$	2.237 (2)	76	1937	76
23	$Fp'(\overline{Si(Ph)(C}H_2)_5)(L)$	2.191 (2)	77	1907[c]	77
24	$[Fp'(CO)(L)]^+[C_2(CN)_4]^-$	2.240 (1)	78	2033	36
25	$Fp''(C(O)Me)(L)$	2.216 (3)	79	1914	80
26	$Fp''(I)(L)$	2.223 (4)	79	1949	79

[a] Abbreviations: L = PPh_3; Ph = C_6H_5; Me = CH_3; Et = C_2H_5; ment = menthyl, cyclohex = cyclohexadiene; DEF = diethyl fumarate; DEM = diethyl maleate; MA = methyl acrylate, TAC = thioacrolein; Fp′ = $(\eta^5\text{-}C_5H_5)Fe(CO)$; Fp″ = $(\eta^5\text{-}(1\text{-Me-3-PhC}_5H_3)Fe(CO)$. [b] Where applicable, values in {} refer to the mean value of l(Fe–P) used to construct the plots. [c] KBr spectrum. [d] See Experimental Section.

Table VI. Comparison of Isoelectronic and Isostructural Pairs of Iron and Manganese Complexes

no.	complex[a]	⟨ν(CO)⟩[b]	Δ(⟨ν(CO)⟩)[b]	l(M–P)[c]	Δ(l(M–P))[c]
		First Group: Fe(CO) → Mn(NO)			
15	$Fe(CO)(NO)_2(L)$	2010		2.260 (3)	
27	$Mn(NO)_3(L)$	...	...	2.315 (2)[d]	+0.055 (3)
6	$Fe(CO)_4(L)$	1980		2.244 (1)	
28	$Mn(CO)_3(NO)(L)$	1977[e]	−3	2.305 (4)[f]	+0.061 (4)
		Second Group: Fe → Mn^-			
6	$Fe(CO)_4(L)$	1980		2.244 (1)	
29	$[Mn(CO)_4(L)]^-[PPN]^+$	1853[g]	−127	2.248 (2)[h]	+0.004 (2)
24	$[Fe(CO)_2(L)(Cp)]^+$	2033		2.240 (1)	
30	$Mn(CO)_2(L)(Cp)$	1897[i]	−136	2.236 (3)[j]	−0.004 (3)
2	$[Fe(CO)_2(NO)(L)_2]^+$	2022		2.280 [3]	
4	$Mn(CO)_2(NO)(L)_2$	1906[e]	−116	2.279 [1][k]	−0.001 (2)

[a] Abbreviations: L = $P(C_6H_5)_3$; Cp = $(\eta^5\text{-}C_5H_5)$. [b] In cm^{-1}. Data taken from Table V, unless stated otherwise. [c] In Å. Data taken from Table V, unless stated otherwise. [d] From ref 54. [e] From ref 70. [f] From ref 81. [g] From ref 82 (IR data relative to the solvent-separated ion pair of the Na^+ salt). [h] From ref 62. [i] From ref 35. [j] From ref 83. [k] From ref 16.

the bond length l(Fe–P) and ⟨ν(CO)⟩.

Results and Discussion

Description of the Structure and Comparison with Its Os and Mn Analogues. The crystal structure consists of discrete $[Fe(CO)_2(NO)(PPh_3)_2]^+$ cations, BF_4^- anions, and CH_2Cl_2 solvent molecules. The structure of cation **2** and the atomic numbering are presented in Figure 1, and selected bond lengths and angles of particular interest are listed in Table III. The coordination around the Fe atom is an almost ideal trigonal bipyramid with the dicarbonyl and nitrosyl forming the basal plane and the P atoms in apical positions. The BF_4^- anion has two preferred orientations about equally occupied, with one common B–F bond. Similarly, the CH_2Cl_2 molecule is disordered in two positions sharing the same C position. The BF_4^- and CH_2Cl_2 are situated in channels between the cations of the unit cell.

The valence angles around the Fe atom of complex **2** are compared in Table IV to the closely related structures $[Os(CO)_2(NO)(PPh_3)_2]^+[ClO_4]^-$ (**3**)[15] and $Mn(CO)_2(NO)(PPh_3)_2$ (**4**),[16] which have similar coordination polyhedra and differ only in the electrical charge and/or the nature of the metal. In cation **2** and cation **3** the CO and NO are statistically distributed in the equatorial plane whereas a localized model was found satisfactory for compound **4**. In the iron cation **2**, the thermal ellipsoids for the phosphorus atoms are normal, indicating that the P atoms are not disordered. It is clear from the P–M–CN and CN–M–CN angles in Table IV that the Fe cation **2** has the best geometrical balance among the equivalent angles, while the Os complex shows an imbalance in the CN–M–CN angles and the Mn complex has imbalance in the P–M–CN angles. The latter complex also contains a P–Mn–P angle of only 170.2 (2)°, while the corresponding angle in the other two compounds (177.45 (5), 177.96 (8)°) is much closer to 180°. The large differences among the basal CN–M–CN angles of the Os complex (115.2, 119.5, 125.3 (5)°) do not occur in the Fe and Mn complexes and seem to result from intermolecular interactions. A simple calculation shows that an intermolecular O(2)···C(13′) distance of 3.110 Å in the Os structure would become 2.92 Å if the CN–Os–CN angles are evened out to ca. 120° each, whereas the shortest O···C contacts are 3.094 (6) and 3.061 (18) Å in the Fe and Mn complexes **2** and **4**, respectively.

In complex **2**, there are no unusual nonbonded contacts involving the ions or solvent molecules. The Fe atom is only −0.008 (1) Å from the mean plane formed by the CN and O atoms. The mean values of 1.762 [6] Å[18] and 1.134 [5] Å for the Fe–CN and CN–O bonds, respectively, are unexceptional when compared to the compilations of Fe–C, Fe–N, and C–O bond lengths given in ref 19–21. The mean value for the CN–O bond lengths also is identical with that of 1.135 [7] Å for $Co(CO)_2(NO)(PPh_3)$, in which a similar CO/NO interchange was encountered.[22]

Comparison of Complexes 1 and 2. This comparison leads to the most interesting results of our study. Two outstanding features are observed from the substitution of CO in **2** by H^- in **1**. First, the two phosphines are displaced from true apical positions so that the P–Fe–P angle of 177.45 (5)° in **2** becomes 140.9 [1]° in hydride **1**. This is accompanied by a small decrease in the mean C–P–C angle from 105.2 [8]° in **2** to 103.4 [18]° in **1**. Second, the mean Fe–P bond is shortened by a substantial amount, from 2.280 [3] Å in **2** to 2.182 [7] Å in **1**. Short M–P bonds and significant deviations from a regular coordination polyhedron have already been reported for other metal hydride complexes[23-26] and have been ascribed partly to the smaller steric requirement of the hydrido ligand (see ref 23 for a recent example).

In compound **1** the angular deformations at Fe result from a substantial shift of the phosphine groups in the direction of the hydride and away from the basal CO and NO. This is indeed in accord with what would be expected from steric considerations, since the hydride has lower steric demand than CO and NO.[29] This shift also has the effect of reducing the apical to basal intramolecular interactions when shorter Fe–P bonds are to be accommodated in the structure. The shift of the phosphine groups, therefore, satisfies these dual steric requirements. In the d^8 trigonal-bipyramidal manganese complexes $Mn(NO)_2(P(OMe)_2Ph)_2X$ (X = Cl, $[P(OMe)_2Ph]^+$)[27,28] minimization of $N_{eq}\cdots P_{ax}$ internal compression strains already has been advocated to rationalize the bending of the axial ligands away from the NO's. The possible factors behind the shorter Fe–P bonds in compound **1** are examined in the reminder of this section.

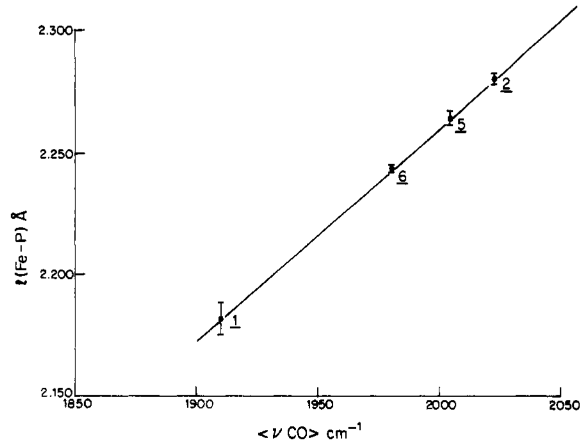

Figure 2. Mean Fe–P bond lengths vs. ⟨ν(CO)⟩ for four closely related trigonal-bipyramidal d^8 complexes.

An estimation of the relative contributions of bonding and nonbonding forces to the bond length changes may be more controversial. For example, the predominant influence of a steric decompression was considered to account for the decrease of l(M–P) by ca. 0.04–0.05 Å upon H for Cl substitution in selected square-planar platinum and octahedral iridium complexes.[23] In contrast, for other square-planar platinum complexes, the predominant influence of electronic factors was suggested for the 0.03–0.05 Å contraction in l(Pt–P) upon H for X (X = Cl, Br) substitution,[33a,34] indicating that the H ligand lies toward the lower end of the cis-influence scale. On that basis, with CO located at the upper end of the same scale,[31,32] it would have been tempting to rationalize the large shortening of Fe–P from **2** to **1** in terms of electronic factors; however, we considered it precarious to apply the results of a third-row element with a different structural type to a first-row metal.

Therefore, in order to seek less ambiguous arguments, we set out to establish the extent of correlation between l(Fe–P) and another parameter known to be influenced predominantly by the electronic properties of the ligands. With metal carbonyls, it is customary to use the carbonyl stretching frequencies ν(CO)'s or the related stretching force constants k(CO)'s (see ref 9 and 35–40

---

[15] Clark, G. R.; Waters, J. M.; Whittle, K. R. *J. Chem. Soc., Dalton Trans.* **1975**, 2233.

[16] Enemark, J. H.; Ibers, J. A. *Inorg. Chem.* **1967**, *6*, 1575.

[17] Pauling, L. "The Nature of the Chemical Bond"; Cornell University Press: Ithaca, NY, 1960; p 260.

[18] Standard deviations for the mean values are calculated as $\sigma(\bar{x}) = [\sum_{i=1}^{n}(x_i - \bar{x})^2/(n-1)]^{1/2}$ to reflect the spread of the measurements and are enclosed in [].

[19] Haymore, B. L.; Ibers, J. A. *Inorg. Chem.* **1975**, *14*, 1369.

[20] Albano, V. G.; Araneo, A.;Bellon, P. L.; Ciani, G.; Manassero, M., *J. Organomet. Chem.* **1974**, *67*, 413.

[21] Feltham, R. D.; Enemark, J. H. *Top. Stereochem.* **1981**, *12*, 155.

[22] Albano, V. G.; Bellon, P. L.; Ciani, G. *J. Organomet. Chem.* **1972**, *36*, 155.

[23] Robertson, G. B.; Tucker, P. A. *J. Am. Chem. Soc.* **1982**, *104*, 318.

[24] Cowie, M.; Haymore, B. L.; Ibers, J. A. *Inorg. Chem.* **1975**, *14*, 2617.

[25] Frenz, B. A.; Ibers, J. A. *Transition Met. Hydrides* **1971**, *1*, Chapter 3.

[26] Whitfield, J. M.; Watkins, F.; Tupper, G. B.; Baddley, W. H. *J. Chem. Soc., Dalton Trans.* **1977**, 407.

[27] Laing, M.; Reiman, R. H.; Singleton, E. *Inorg. Chem.* **1979**, *18*, 324.

[28] Laing, M.; Reiman, R. H.; Singleton, E. *Inorg. Chem.* **1979**, *18*, 2666.

[29] From ref 30 the cone angles for various ligands are as follows: H, 75°; CO, ~95°; NO, ~95°; Cl, ≃102°; PPh_3, 145°.

[30] Tolman, C. A. *Chem. Rev.* **1977**, *77*, 313.

[31] Manojlović-Muir, L.; Muir, K. W.; Solomun, T. *J. Organomet. Chem.* **1977**, *142*, 265.

[32] Cairns, M. A.; Dixon, K. R.; Rivett, G. A. *J. Organomet. Chem.* **1979**, *171*, 373.

[33] (a) Hitchcock, P. B.; Jacobson, B.; Pidcock, A. *J. Chem. Soc., Dalton Trans.* **1977**, 2038. (b) *Ibid.* **1977**, 2043.

[34] Delpra, A.; Forsellini, E.; Bombieri, G.; Michelin, R. A.; Ross, R. *J. Chem. Soc., Dalton Trans.* **1979**, 1862.

[35] Connelly, N. G.; Kitchen, M. *J. Chem. Soc., Dalton Trans.* **1977**, 931.

[36] Long, G. J.; Alway, D. G.; Barnett, K. W. *Inorg. Chem.* **1978**, *17*, 486.

[37] Jolly, W. L.; Avanzino, S.; Rietz, R. R. *Inorg. Chem.* **1977**, *16*, 964.

[38] Bodner, G. M.; May, P. M.; McKinney, L. E. *Inorg. Chem.* **1980**, *19*, 1951 and references therein.

[39] King, R. B. *Inorg. Chim. Acta* **1968**, *2*, 454.

[40] Cutler, A.; Raghu, S.; Rosenblum, M. *J. Organomet. Chem.* **1974**, *77*, 381.

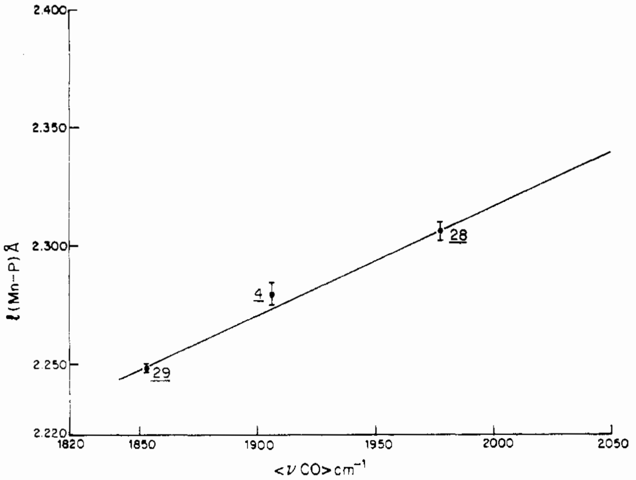

Figure 3. Mean Mn–P bond lengths vs. ⟨ν(CO)⟩ for three closely related trigonal-bipyramidal d^8 complexes.

for a variety of correlations with these parameters). For example, the variations in ν(CO)'s upon a ligand substitution are caused primarily by the difference in the donor/acceptor properties of the exchanged ligands[41-43] and generally are regarded as reflecting predominantly a change in the metal to CO back-bonding.[44] In the present study, we chose the degeneracy-weighted stretching frequency ⟨ν(CO)⟩, which has been used already as a convenient substitute for the CO stretching force constants.[37,40]

A literature search of the Cambridge Crystallographic Data File[46] for iron carbonyl triphenylphosphine complexes was carried out on the Jan 1983 release. Structural data for the 24 compounds resulting from this search[47] are presented in Table V, together with the corresponding ⟨ν(CO)⟩ values, and are considered to be an adequate sample for this study. The ⟨ν(CO)⟩ values were computed from literature data, some of which likely were obtained by routine measurements and may include uncertainties of 5–10 cm^{-1}. The list in Table V represents a variety of monometallic, coordinatively saturated complexes with a $Fe(CO)(PPh_3)$ subunit. The Fe–P bond lengths in the present compilation differ by as much as 0.12 Å, i.e. double the largest difference in a previous compilation.[48] Fe–P bonds even longer than those listed in Table V have been reported, e.g. 2.339 (2) Å in $Fe(NO)_2(PPh_3)Cl$[49] and 2.310 (3) Å in $[Fe(p\text{-tolyl-NC})_3(PPh_3)_2Cl]^+$,[50] but these have been excluded due to the absence of a CO ligand. As shown in Table V, the two complexes of prime interest **1** and **2** have Fe–P bond lengths close to the lower and upper limits of the present compilation.

Complexes **1** and **2** form with $[Fe(CO)_2(N_2Ph)(PPh_3)_2]^+$ (**5**) and $Fe(CO)_4(PPh_3)$ (**6**) a series of closely related trigonal-bipyramidal d^8 complexes. Each member is related to cation **2** by a formal single or double ligand substitution. $Fe(CO)_3(PPh_3)_2$ would have been valuable to complete the set, but its structure is not available. The mean Fe–P bond lengths vs. ⟨ν(CO)⟩ of this series are shown in Figure 2 to form an almost perfectly linear relationship, with a positive slope ($r = 0.9999$, σ(Fe–P) (standard error of the estimate) = 0.0005 Å). However, the exact linearity probably is fortuitous as a result of averaging the bond lengths in each of complexes **1**, **2**, and **5**.

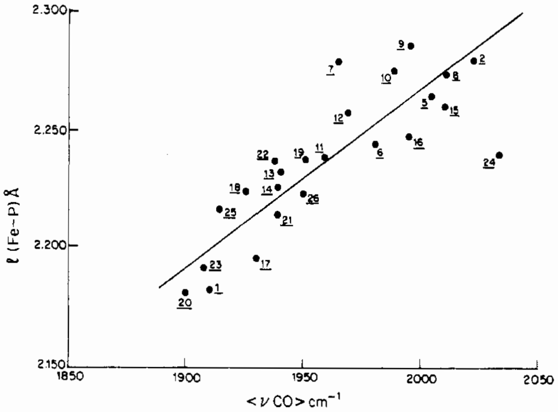

Figure 4. Distribution of the mean Fe–P bond lengths vs. ⟨ν(CO)⟩ for the 24 widely varied Fe complexes listed in Table V.

From this result, we conclude that, upon going from cation **2** to hydride **1**, the variation in *l*(Fe–P) correlates well with the changes in the ligand electronic properties from CO to H^-. Therefore, we rationalize the observed change as a consequence of both the electronic properties of H^- relative to CO, which favors a shortening of *l*(Fe–P), and the steric requirement of the H ligand, which allows the angular deformations required for shorter metal–phosphine bonds.

The series of trigonal-bipyramidal d^8 manganese complexes comprising $Mn(CO)_2(NO)(PPh_3)_2$ (**4**), $Mn(CO)_3(NO)(PPh_3)$ (**28**), and $[Mn(CO)_4(PPh_3)]^-$ (**29**) (Table VI) also is of interest. Starting with compound **28**, a single ligand substitution yields each of the other two members of the set. Furthermore, in that case the steric demand of the basal ligand remains comparable.[29] The *l*(Mn–P) vs. ⟨ν(CO)⟩ plot presented in Figure 3 (data taken from Table VI) indicates that the same kind of relationship exists between *l*(Mn–P) and ⟨ν(CO)⟩. It should be noted further that the decrease in *l*(Mn–P) from **28** to **4** upon PPh_3 for trans CO substitution parallels the shortening of the Cr–P bonds from $Cr(CO)_5(P(OPh)_3)$ (2.309 (1) Å) to *trans*-$Cr(CO)_4(P(OPh)_3)_2$ (2.252 (1) Å).[51] In contrast, from $Mo(CO)_5(PPh_3)$ to *cis*-$Mo(CO)_4(PPh_3)_2$, *l*(Mo–P) increases by 0.017 (2) Å.[52] However, in the disubstituted molybdenum derivative, the large opening of the P–Mo–P angle from the regular value of 90° to 104.63 (7)° indicates severe nonbonded interactions between the two phosphines.

The distribution of the mean *l*(Fe–P) vs. ⟨ν(CO)⟩ for the 24 widely varied iron complexes listed in Table V is presented in Figure 4. Except for compounds **7** and **24**, the other 22 complexes show an acceptable linear correlation ($r = 0.9149$, σ(Fe–P) = 0.0123 Å) with maximum deviations of ±0.02 Å from the regression line. Thus, even if the relationship is far from being quantitative, the general trend for *l*(Fe–P) to increase with ⟨ν(CO)⟩ still is quite obvious for most of the compounds. Although explanation of the finer details of this distribution can be only speculative at this time, it may be worthwile to single out the pair of cyclopentadienyl derivatives $(\eta^5\text{-}C_5H_5)Fe(CO)(PPh_3)$–R with R = CH_2CO_2-menthyl (**17**) (Fe–P = 2.196 [4] Å, ⟨ν(CO)⟩ = 1930 cm^{-1}) and R = $C(CO_2Et)CMe_2$ (**18**) (Fe–P = 2.2336 (6) Å, ⟨ν(CO)⟩ = 1925 cm^{-1}). The ⟨ν(CO)⟩ values are close but the Fe–P distances differ by 0.038 (3) Å, which is significant to the extent of 12σ. For **18**, evidence was presented for nonbonded

---

(41) Tolman, C. A. *J. Am. Chem. Soc.* **1970**, *92*, 2953.

(42) Horrocks, W. D., Jr.; Taylor, R. C. *Inorg. Chem.* **1963**, *2*, 723.

(43) (a) Graham, W. A. G. *Inorg. Chem.* **1968**, *7*, 315. (b) Brown, R. A.; Dobson, G. R., Inorg. *Chim. Acta* **1972**, *6*, 65. (c) King, R. B.; Houk, L. W. *Can. J. Chem.* **1969**, *47*, 2959.

(44) See ref 36–38 and 45.

(45) Chen, H. W.; Jolly, W. L. *Inorg. Chem.* **1979**, *18*, 2548.

(46) Allen, F. H.; Bellard, S.; Brice, M. D.; Cartwright, B. A.; Doubleday, A.; Higgs, H.; Hummelink, T.; Hummelink-Peters, B. G.; Kennard, O.; Motherwell, W. D. S.; Rodgers, J. R.; Watson, D. G., *Acta Crystallogr., Sect. B:. Struct. Crystallogr. Cryst. Chem.* **1979**, *B35*, 2331.

(47) In Table V are listed only complexes for which both *l*(Fe–P) and ν(CO) values are available. Furthermore, structures with σ(M–P) ≥ 0.01 Å were not considered.

(48) Reisner, G. M.; Bernal, I.; Brunner, H.; Muschiol, M. *Inorg. Chem.* **1977**, *17*, 783.

(49) Kopf, J.; Schmidt, J. *Z. Naturforsch. B: Anorg. Chem., Org. Chem.* **1975**, *30B*, 149.

(50) Pelizzi, G.; Albertino, G.; Bordignon, E.; Orio, A. A.; Calogero, S. *Acta Crystallogr., Sect. B: Struct. Crystallogr. Cryst. Chem.* **1977**, *B33*, 3761.

(51) (a) Preston, H. S.; Stewart, J. M.; Plastas, H. J.; Grim, O. S. *Inorg. Chem.* **1972**, *11*, 161. (b) Plastas, H. J.; Stewart, J. M. Grim, O. S. *Inorg. Chem.* **1973**, *12*, 265.

(52) Cotton, F. A.; Darensbourg, D. J.; Klein, S.; Kolthammer, B. W. S. *Inorg. Chem.* **1982**, *21*, 294.

interactions between PPh_3 and ligand R,[53] indicating that the phosphine is in a more crowded environment than in **17**. It may be possible then that steric factors have a more important role in controlling the Fe–P separation in **18** relative to that in **17**.

Comparison of Isoelectronic and Isostructural Mn and Fe Complexes. Other observations of relevance to the present discussion are obtained by comparing pairs of isoelectronic and isostructural Fe and Mn complexes. They are listed in Table VI in two separate groups, the first representing the replacement of Fe(CO) by Mn(NO) and the second is for the replacement of Fe by Mn^-. In the first group, the metal–phosphorus distances are 0.055–0.061 Å longer in the manganese derivative relative to the iron complex. For the pair of complexes **15** and **27**, an expansion of the metal σ-covalent radius has already been suggested as a factor contributing to the lengthening.[54] The same reason could apply equally well for the second pair **6** and **28**. In sharp contrast, the M–P bond lengths in each pair of the second group remain virtually unchanged (Table VI). Therefore, an additional and efficient factor must counterbalance the postulated metal size effect. Considering only the perturbations affecting the M–P σ bonds, we have been unable to identify influences specific to the second group which could rationalize this difference in behavior. For each pair of the second group, replacement of Fe by Mn^- leaves unaffected the identity of the supporting ligands, but the electric charge increases by one negative unit. In every case, the large decrease in $\langle\nu(\mathrm{CO})\rangle$ is indicative of a notable increase in back-bonding from the metal to the π-acid ligands. Accepting PPh_3 as one of them (see ref 55 and 56 for supporting arguments), albeit a weaker one than CO,[57] then if an increase in the M–P multiple bond character actually occurs, it might contribute to a shortening of the bond. That would introduce a factor in the right direction to oppose the effect of the metal change, provided that the first group of compounds is lacking this potential influence. In each pair of the first group, upon going from the iron to the manganese complex, the overall electrical charge remains the same but one CO is converted into NO. Again the availability of π electrons is expected to increase from Fe to Mn.[37,45] However, evidence has been presented for the strong competitive effect NO may have on the repartitioning of π electrons between the ligands. This competition culminates in depleting the electron density of the M–C(O) π bonds upon going from $Fe(CO)_2(NO)_2$ to $Mn(CO)(NO)_3$.[45] The weaker π acidity of PPh_3 relative to CO strongly suggests that the M–P bond order also should decrease from $Fe(CO)(NO)_2(PPh_3)$ (**15**) to $Mn(NO)_3(PPh_3)$ (**27**). Whether or not this effect could add significantly to the lengthening of l(M–P) is not known. Alternatively, no adverse effect was visible from $Fe(CO)_5$ to $Mn(CO)_4(NO)$[45] (as well as in all of the nitrosyl compounds considered in the first part of this discussion). However, competition does surface again upon going from $Fe(CO)_4(PPh_3)$ (**6**) to $Mn(CO)_3(NO)(PPh_3)$ (**28**). The lack of a significant variation in $\langle\nu(\mathrm{CO})\rangle$ (Table VI) is an indication that the CO ligands benefit very little from changing the metal. If NO is strong enough to prevent an increase in back-bonding toward CO upon going from **6** to **28**, the effect should be even stronger on PPh_3, the weakest π acid. It follows that back-bonding toward PPh_3 should not increase significantly on going from the iron to the manganese complex. Therefore, the most straightforward rationalization of the relative changes in l(M–P) for these two families of complexes is the enhancement of π bonding toward PPh_3 upon replacement of Fe by Mn in the (Fe, Mn^-) group compared to the [Fe(CO), Mn(NO)] group.[84]

In each series of compounds considered in the l(M–P) vs. $\langle\nu(\mathrm{CO})\rangle$ plots, rationalization of the positive correlation between l(M–P) and $\langle\nu(\mathrm{CO})\rangle$ is readily attributable to a significant influence of the multiple-bond character on l(M–P); however, if back-bonding does play a role, it is evidently not the sole electronic factor involved. Since the metal σ-covalent radius is influenced not only by the metal oxidation state but also by its coordination number and the extent of depature of the coordination polyhedron from regular geometry, it is expected that alteration of the σ-electron framework contributes to the modification of l(M–P).[59] The situation is further complicated by the participation of steric factors that, in selected cases, may offset the electronic influences, resulting in deviations from the general trends.

Conclusions. H^- for CO substitution in cation **2** to afford hydride **1** shortens the Fe–P bonds by ca. 0.1 Å and reduces the P–Fe–P angle by ca. 36°. The change in bond lengths has been attributed primarily to the difference in the electronic properties

---

(53) Reger, D. L.; McElligot, P. J.; Charles, N. G.; Griffith, E. A. H.; Amma, E. L. *Organometallics* **1982**, *1*, 443.

(54) Wilson, R. D.; Bau, R. *J. Organomet. Chem.* **1980**, *191*, 123.

(55) Gerloch, M.; Hanton, L. R. *Inorg. Chem.* **1981**, *20*, 1046.

(56) Gerloch, M.; Mason, R. *Inorg. Chim. Acta* **1981**, *50*, 43.

(57) See ref 43. In extreme situations, such as in $[Fe(CO)_n(PPh_3)_{3-n}(\eta^5\text{–}C_5H_5)]^+$ (n = 1, 2), metal to PPh_3 back-bonding was considered negligible relative to back-bonding to CO.[58]

(58) Johnson, B. J.; Ouseph, P. J.; Hsieh, J. S.; Steinmetz, A. L.; Shade, J. E. *Inorg. Chem.* **1979**, *18*, 1796.

(59) Mason, R.; Meek, D. W. *Angew. Chem., Int. Ed. Engl.* **1978**, *17*, 183.

(60) Johnson, B. F. G.; Segal, J. A. *J. Chem. Soc., Dalton Trans.* **1972**, 1268.

(61) Carroll, W. E.; Lalor, F. J. *J. Chem. Soc., Dalton Trans* **1973**, 1754.

(62) Riley, P. E.; Davis, R. E. *Inorg. Chem.* **1980**, *19*, 159.

(63) Le Bozec, H.; Dixneuf, P. H.; Carty, A. J.; Taylor, N. J. *Inorg. Chem.* **1978**, *17*, 2568.

(64) Professor J. Takats, personal communication.

(65) Harlow, R. L.; Pfluger, C. E. *Acta Crystallogr., Sect. B: Struct. Crystallogr. Cryst. Chem.* **1973**, *B29*, 2633.

(66) Professor C. Dittmer, personal communication.

(67) Sacerdoti, M.; Bertolasi, U.; Gilli, G. *Acta Crystallogr., Sect. B: Struct. Crystallogr. Cryst. Chem.* 1981, *B36*, 1061.

(68) Cardacci, G.; Bella Chioma, G. *Inorg. Chem.* **1977**, *16*, 3099.

(69) Pearson, A. J.; Raithby, P. R. *J. Chem. Soc., Dalton Trans.* **1981**, 884.

(70) Beck, W.; Lottes, K. *Chem. Ber.* **1965**, *98*, 2657.

(71) Mitsudo, T. A.; Sasaki, J.; Watanabe, Y.; Takegami, Y.; Nishigaki, S.; Nakatsu, K. *J. Chem. Soc., Chem. Commun.* **1978**, 252.

(72) Chou, C. K.; Miles, D. L.; Bau, R.; Flood, T. C. *J. Am. Chem. Soc.* **1978**, 100, 7271.

(73) Flood, J. C.; Disanti, F. J.; Miles D. L. *Inorg. Chem.* **1976**, *15*, 1910.

(74) Miles, S. L.; Miles, D. L. Bau, R.; Flood, J. C. *J. Am. Chem. Soc.* **1978**, *100*, 7278.

(75) Brunner, H.; Schmidt, E. *J. Organomet. Chem.* **1973**, *50*, 219.

(76) Boland-Lussier, B. E.; Churchill, M. R.; Hughes, R. P.; Rheingold, A. L. *Organometallics* **1982**, *1*, 628.

(77) Holmes-Smith, R. D.; Stobart, S. R.; Atwood, J. L.; Hunter, W. E. *J. Chem. Soc., Dalton Trans.* **1982**, 2461.

(78) Sim, G. A.; Woodhouse, D. I.; Knox, G. R. *J. Chem. Soc., Dalton Trans.* **1979**, 629.

(79) Attig, T. G.; Teller, T. G.; Wu, S. M.; Bau, R.; Wojcicki, A. *J. Am. Chem. Soc.* **1979**, *101*, 619.

(80) Attig, T. G.; Wojcicki, A. *J. Organomet. Chem.* **1974**, *82*, 397.

(81) Enemark, J. H.; Ibers, J. A. *Inorg. Chem.* **1968**, *7*, 2339.

(82) York, Darensbourg, M.; Darensbourg, P. J.; Burns, D; Drew, D. A. *J. Am. Chem. Soc.* **1976**, *98*, 3127.

(83) Barbeau, C.; Dichman, K. S.; Ricard, L. *Can. J. Chem.* **1973**, *51*, 3027.

(84) The alternative approach would be to postulate a priori that PPh_3 is not involved at all in back-bonding, on the basis that in metal phosphine compounds "there seems to be no instance where back-bonding is required to explain the observed physical properties"[85] (but see ref 55 and 56). As suggested by a reviewer, a hypothesis that is worthy of consideration is that for each pair of the (Fe, Mn^-) group, the CO's remove the electron density from Mn^- so that it functions much like Fe. For the pair of complexes **6** and **29** belonging to that group (see Table VI), we can go from **6** to **28** (Δl(M–P) > 0) and then from **28** to **29** (Δl(M–P) < 0). In line with this hypothesis, we should conclude that the shortening of Mn–P for the latter pair is also the result of enhanced back-bonding toward the CO's, which, by causing an increase in the effective nuclear charge perceived by the metal valence electrons, allows the metal σ-covalent radius to contract. Although the effect of a single ligand substitution (i.e. CO for NO^+ from **28** to **29**) on the metal electric charge is difficult to assess, Mössbauer spectroscopy with iron complexes tends to indicate that the change at the metal is likely to be minimal. Hence, the effect on the metal covalent radius is small, provided that at least three good π acceptors are present in the metal coordination sphere.[58] The fulfillment of this condition in compounds **28** and **29** leads us to discard this hypothesis.

(85) Collman, J. P., Hegedus, L. S., Eds. "Principles and Applications of Organotransition Metal Chemistry"; University Science Books: Mill Valley, CA, 1980; pp 54–55.

of H$^-$ and CO. The angular deformations have been rationalized in terms of steric effects. Furthermore, in the three series of complexes studied, the general tendency of l(M-P) to vary in the same direction as $\langle\nu(\mathrm{CO})\rangle$ indicates that an increase in the metal Lewis basicity, as inferred from a decrease in $\langle\nu(\mathrm{CO})\rangle$, favors a shortening of the M-P bonds. Our interpretation of the bond length variations is that π bonding might provide a substantial contribution to the changes observed.

Acknowledgment. The authors wish to thank Professors J. Takats and C. Dittmer for providing the IR data pertaining to complexes **8**, **9** and **11**, M. E. Pippy for assistance with the computations, and the Natural Sciences and Engineering Research Council of Canada for financial support to J.L.A.R.

Registry No. $[\mathrm{Fe(P(C_6H_5)_3)_2(CO)_2(NO)}]^+[\mathrm{BF_4}]^-\cdot\mathrm{CH_2Cl_2}$, 96689-06-4.

Supplementary Material Available: Listings of observed and calculated structure factors, anisotropic thermal parameters for the non-hydrogen atoms, and the geometries of the phenyl rings, disordered BF_4^- anion, and CH_2Cl_2 solvent molecule (32 pages). Ordering information is given on any current masthead page.

Contribution from the Institute of Inorganic Chemistry,
University of Munich, D-8000 Munich 2, Federal Republic of Germany

Competition between Adduct and Cation Formation in Reactions between Diorganylborane Derivatives and Pyridine or Lutidines[1]

CHAITANYA K. NARULA[†] and HEINRICH NÖTH*

Received October 9, 1984

1:1 coordination compounds are formed in the reaction of pyridine and 2,4-lutidine with dibutylboron triflate, 9-(((trifluoromethyl)sulfonyl)oxy)-9-borabicyclo[3.3.1]nonane, and 9-(((trifluoromethyl)sulfonyl)oxy)-9-borafluorene. In contrast, 2,6-lutidine yields the borenium(1+) triflates **1a**,**b**, with the first two boron triflates. Neutral addition compounds result from the three bases and dibutylboron chloride, 9-chloro-9-borabicyclo[3.3.1]nonane, and 9-chloro-9-borafluorene, respectively. Their interaction with $GaCl_3$ or $AlCl_3$ as chloride acceptors leads to nitrogen base exchange in most cases, but $GaCl_3$ abstracts Cl$^-$ from 9-chloro-9-borafluorene–pyridine ($C_{17}H_{13}BClN$, triclinic, $a = 9.721$ (2) Å, $b = 11.439$ (2) Å, $c = 13.767$ (3) Å, $\alpha = 92.55$ (2)°, $\beta = 103.27$ (2)°, $\gamma = 105.46$ (6)°, space group $P\bar{1}$, $Z = 4$) to form the red 9-borafluorenium tetrachlorogallate–pyridine compound **12**, while 9-chloro-9-borafluorene–acridine and aluminum chloride yield the dark red tetrachloroaluminate **14**, whose structure has been determined by X-ray crystallography ($C_{25}H_{17}AlBCl_4N$, triclinic, $a = 9.401$ (5) Å, $b = 9.621$ (6) Å, $c = 16.183$ (9) Å, $\alpha = 103.71$ (5)°, $\beta = 92.86$ (4)°, $\gamma = 117.15$ (4)°, space group $P\bar{1}$, $Z = 2$). The cation in **14** shows almost planar acridine and 9-borafluorene moieties, whose planes form an interplanar angle of 62°. Characteristic for the cation are short B–C bonds (1.46 Å) and a very long C–C single bond (1.66 Å) of the five-membered borole ring. The formation of base-stabilized diorganylborenium(1+) ions depends on steric and electronic effects.

Introduction

Recent studies have firmly established the existence of tricoordinated borenium salts of type A–C.[2-4] Obviously, the nitrogen atoms help to stabilize these cations by π back-bonding to boron, thus delocalizing the positive charge. This effect decreases as the amino groups are replaced by aryl or alkyl groups, and consequently, salts containing cations of type $R_2N(R')BL^+$ (L = ligand) are considerably less stable.[5] Our current interest in tricoordinated borenium salts, which results from attempts to better understand the mechanism of substitution at tricoordinated boron atoms, and scanty reports on these ions in the literature,[6-8] the majority of which have been found by us to be incorrect,[9] prompted us to study reactions between selected diorganylborane derivatives and suitable donor molecules in order to find limiting factors for the competition between adduct and salt formation according to eq 1.

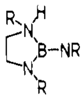
A

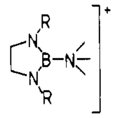
B

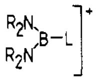
C

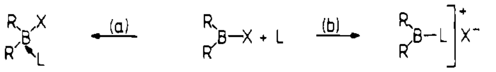

(1)

Experimental Section

All experimental manipulations were conducted under rigorously anhydrous conditions in a high-vacuum system and/or by the Schlenk tube technique in an oxygen-free nitrogen atmosphere. Solvents were dried by standard techniques and stored under nitrogen. Pyridine, 2,4- and 2,6-lutidine, and acridine were commercial products. They were dried, distilled, or recrystallized before use. Trifluoromethanesulfonic acid and silver triflate were purchased from Fluka Corp. and used as supplied. Dibutylboron triflate and 9-(((trifluoromethyl)sulfonyl)oxy)-9-borabicyclo[3.3.1]nonane were prepared according to literature procedures,[10] and the same holds for the chlorides.[10] The 9-borafluorene derivatives have been obtained via *o,o'*-biphenylmercury and BCl_3.[11]

NMR spectra were recorded on a JEOL FX 90 or a Bruker WP 200 PFT multinuclei NMR spectrometer. Chemical shifts refer to Me_4Si (^1H) and $BF_3\cdot OEt_2$ (^{11}B), respectively. Positive δ values correspond to frequencies higher than the standard. A SYNTEX R3 automated four-circle diffractometer was used for intensity data collection, and computations were performed on a NOVA 3 computer using SHELXTL programs. Elemental analyses were obtained from the Institute's microanalytical laboratory.

General Procedure. A solution of the diorganylborane was cooled to −78 °C, and the solution of the base, usually in the same solvent, was

---

[†] Aldexander von-Humboldt Fellow.

(1) Contribution to the Chemistry of Boron. 150. For contribution 149 in this series see ref 3.
(2) Narula, C. K.; Nöth, H. *Inorg. Chem.* **1984**, *23*, 4147.
(3) Narula, C. K.; Nöth, H. *J. Chem. Soc., Chem. Commun.* **1984**, 1023.
(4) Nöth, H.; Rasthofer, B., unpublished results. See also: Rasthofer, B. Dissertation, University of Munich, 1984.
(5) An example of this type is $[\mathrm{tmpB(CH_3)py}]\mathrm{AlCl_4}$ (tmp = 2,2,6,6-tetramethylpiperidino), which decomposes at −20 °C. Weber, S. Thesis, University of Munich, 1981.
(6) Davidson, J. M.; French, C. M. *J. Chem. Soc.* **1958**, *144*; **1962**, 3364. Moodie, R. B.; Elliel, B. *Chem. Ind.* (*London*) **1966**, 761. Armstrong, D. R.; Perkins, P. G. *J. Chem. Soc. A* **1966**, 1026.
(7) Köster, R. "Houben-Weyl, Methoden der Organischen Chemie", 4th ed.; G. Thieme: Stuttgart, New York, 1983; Vol. 13/3b, p 414.
(8) Shchegoleva, T. A.; Mikhailov, B. M. *Izv. Akad. Nauk SSSR, Ser. Khim.* **1965**, 714.
(9) Narula, C. K.; Nöth, H. *Z. Naturforsch., B*: *Anorg. Chem., Org. Chem.* **1983**, *B38*, 1161. See also unpublished results for these authors.
(10) Evans, D. A.; Nelson, J. V.; Vogel, E.; Taber, T. R. *J. Am. Chem. Soc.* **1981**, *103*, 3099.
(11) Narula, C. K.; Nöth, H. *J. Organomet. Chem.* **1985**, *281*, 131.

0020-1669/85/1324-2532$01.50/0 © 1985 American Chemical Society